The Astrophysical Journal, 677:699–703, 2008 April 10

MAGNETIC INTERACTION: A TRANSEQUATORIAL JET AND INTERCONNECTING LOOPS

Yunchun Jiang,[1] Yuandeng Shen,[1] Bi Yi,[1] Jiayan Yang,[1] and Jingxiu Wang[2]

Received 2007 June 28; accepted 2008 January 8

ABSTRACT

We present, to our knowledge for the first time, a rare observation of direct magnetic interaction between a transequatorial jet and interconnecting loops (IL) in the southern hemisphere. The jet originated from a flare and appeared to move outward along open field lines, but it passed so close to the IL that its edge met with one of the IL ends. As a result, the IL began to erupt, weak brightenings appeared at the meeting site, and a nearby dark feature was disturbed. After the eruption, in addition to a looplike dimming due to the disappearance of the IL, a dimming region was formed around its another end, which was very probably caused by the expansion or opening of its field lines and represented its evacuated feet. Two coronal mass ejections (CMEs) were observed within 2 hr in association with the event. One was related to the flare and the jet, while the other was due to the IL eruption. These observations suggest that a sole flare can not only trigger a CME but also simultaneously trigger an IL eruption by means of its interaction with a jet, so can lead to two interdependent CMEs, i.e., a sympathetic CME pair physically connected by the jet/IL interaction.

Subject headings: Sun: activity — Sun: coronal mass ejections (CMEs) — Sun: flares — Sun: magnetic fields — Sun: UV radiation

1. INTRODUCTION

Coronal loops are ubiquitous in the solar corona except in coronal holes. They show bright emission in soft X-ray and EUV wavelengths and represent closed magnetic field lines filled with hotter and denser plasma than that of the background corona (Aschwanden 2004). One type of loop is an interconnecting loop (IL) system joining separate active regions (ARs), including large-scale transequatorial interconnecting loop (TIL) system connecting ARs on opposite solar hemisphere (Chase et al. 1976; Pevtsov 2000). The activity of ILs can link two sympathetic flares (Wang et al. 2001), while disturbances and eruptions of TILs, which were often followed by the formation of coronal dimmings, could be closely associated with sympathetic flares, coronal mass ejections (CMEs) and intense geomagnetic storms (Delannée & Aulanier 1999; Pohjolainen et al. 2001; Moon et al. 2002; Glover et al. 2003; Harra et al. 2003; Balasubramaniam et al. 2005; Zhou et al. 2006; Saito et al. 2007; Wang et al. 2007). In particular, Khan & Hudson (2000) presented evidence that the disappearances of TILs can be sources of certain CMEs, which confirmed beyond any doubt the earlier inference from Kahler (1991) that ILs and TILs could erupt to form CMEs. Although the TIL events are only a small minority of the CME precursors in the low corona, they represent a new, specific class of CME origins that do not fit the standard CME model (Hudson & Cliver 2001; Svestka 2001; Cliver & Hudson 2002). Khan & Hudson (2000) also suggested that the TILs were destabilized by flare-generated shock waves impinging on one footpoint of the TILs. In the complex corona, however, the ubiquitous loops stand a very good chance to meet with other erupting magnetic structures. Different from the case of Khan & Hudson (2000), one expects that magnetic interactions between them may lead to eruptions of the loops, and it is clear that observational identification of such interaction is important in understanding destabilization of loops. On the other hand, when multiple, homologous (recurrent) CMEs, which respectively eject from the same active region, have been studied in some events (Lyons & Simnett 1999; Nitta & Hudson 2001; Zhang & Wang 2002; Chertok et al. 2004), sympathetic (interdependent) CMEs, a pair of successive CMEs almost simultaneously originating from different regions with a certain physical connection, were very rarely observed. Only a few plausible sympathetic CME pairs have been reported up until now, and their possible driving mechanism remains greatly unclear (Simnett & Hudson 1997; Moon et al. 2003; Cheng et al. 2005). Detailed investigations of magnetic interaction between two distinct erupting structures will provide clues to understand the occurrence of sympathetic CMEs.

On 2004 July 23, an IL in the southern hemisphere was hit at one end by a transequatorial jet from a flare in the opposite hemisphere. As a result, the IL completely erupted and a dimming region formed around its other end. Just as Jiang et al. (2007d) recently found a the new form of magnetic interaction between an erupting filament and a coronal hole, this paper, the second of a series, presents first evidence for another new type of magnetic interactions occurring between the IL and the flare-associated jet. We further show that the erupting IL and the resultant dimming were sources of a CME, and that definite sympathetic CMEs, consisting of this CME and another CME related to the flare, were physically connected by the jet/IL interaction.

2. OBSERVATIONS

The observations used in the present study include the following:

1. Full-disk He I 10830 Å intensity and velocity images from the Chromospheric Helium Imaging Photometer (CHIP; MacQueen et al. 1998) at the Mauna Loa Solar Observatory (MLSO). The CHIP data are acquired at seven filter positions covering the spectral region from 10826 to 10834 Å, which provide a measure of the line-of-sight velocity component over the range of ± 100 km s^{-1} with an accuracy of approximately ± 5 km s^{-1} (de Toma et al. 2005).

2. Full-disk Hα images from Big Bear Solar Observatory (BBSO) in the USA, one station of the global Hα network (Steinegger et al. 2000). The image cadence is 1 minute, and the pixel size is roughly 1″. On 2004 July 23, BBSO provided Hα

[1] National Astronomical Observatory/Yunnan Astronomical Observatory, Chinese Academy of Sciences, P.O. Box 110, Kunming 650011, China; jyc@ynao.ac.cn.

[2] National Astronomical Observatory, Chinese Academy of Sciences, Beijing 100012, China.

center and −0.6 Å off-band images before and after 16:15 UT, respectively.

3. Full-disk EUV images with a pixel resolution of 2.6″, full-disk line-of-sight magnetograms with a pixel size of 2″ and a cadence of 96 minutes, and the C2 (C3) white-light coronagraph data that cover the range 2 (4) to 6 (32) solar radii, from the Extreme Ultraviolet Telescope (EIT; Delaboudiniére et al. 1995), the Michelson Doppler Imager (MDI; Scherrer et al. 1995), and the Large Angle and Spectrometric Coronagraphs (LASCO; Brueckner et al. 1995) aboard the *Solar and Heliospheric Observatory* (*SOHO*), respectively. EIT 195 Å images were obtained continuously with a cadence of 12 minute, while 171, 284, and 304 Å images were taken only once every 6 hr.

4. Full-disk soft X-ray (SXR) images in the wavelength range of 6–60 Å (sensitive to temperatures of 10^6–10^7 K) with a resolution of 5″ pixel^{-1} from the Solar X-Ray Imager (SXI; Hill et al. 2005) aboard the *GOES-12* satellite. SXR images observed with the polyimide thin filter position were available at a cadence of 4 minutes.

3. RESULTS

The interconnecting loop system connected AR 10653 (S12°, W09°) to a region west of it, while a flare of X-ray class M2.2 occurred in AR 10652 (N08°, W08°) and had start, peak, and end times around 17:07, 17:28, and 17:35 UT, respectively. Figures 1*a* and 1*b* show a MDI magnetogram and an EIT 195 Å image before the flare. A looplike structure, "IL," completely located in the southern hemisphere, had a well-defined semicircular shape with a length of about 3.9×10^5 km. Its eastern end is rooted in the negative-polarity region of AR 10653, while the western end is in extremely weak fields outside this AR. However, some leglike bright features also appeared in the vicinity of the both IL ends (Fig. 1*b*, *arrows*). Besides the IL, therefore, the interconnecting loop system seems to include other loops on the south of the IL, which appeared to be only partially filled so that only their footpoints were bright. The whole loop system showed a characteristic horse-shoe shape and probably consisted of bundles of many loops sharing the same footpoints (Reale 1999).

A distinct characteristic of the event is the entire IL eruption due to a direct interaction with a plasma ejection, a jet in EUV and SXR, originating from the flare in the northern hemisphere. This was quite obvious in the EIT 195 Å fixed-base difference images in Figure 1, which are obtained by subtracting a preflare image. At 17:23 UT during the flare's rise phase, the jet spurted out from a positive polarity region toward the western IL end, and the IL was activated. The jet was a transequatorial one, which traveled a long distance and flowed across the equator. At 17:36 UT after the flare end, the jet passed through the western IL end. Panel *c3* in Figure 1 clearly shows that its southern edge met with this IL end. Although major portions of the jet did not stop but went beyond this end and appeared to eject to space along open field lines (panels *c*3 and *c*4, *arrows*), the timings of the jet and the IL activation make us believe that direct magnetic interaction indeed occurred between them and the IL eruption was clearly the result of such interaction. This was further evidenced by the following appearance of weak brightenings,"WB", around the meeting site (see panels *c*4–*c*6). Thus, magnetic reconnection very likely occurred between the magnetic fields of the jet and the IL. Afterward, the IL continued to rise and finally became invisible after 08:12 UT. The IL eruption thus lasted at least 37 minutes from 17:23 to 18:00 UT, with an average speed (acceleration) of about 41 km s^{-1} (3 m s^{-2}), which was largely lower than the estimated jet average speed of about 200 km s^{-1}. It is also noted that the jet was much brighter than the erupting IL, possibly suggesting that its density was significantly higher than that of the IL. In Figure 1*a* the inferred field line directions of the jet and the IL are indicated by the black curves with arrows, and the outlines of the IL's outermost edges at four times (16:35, 17:36, 17:48, and 18:00 UT) show that the IL eruption was toward the southwestern direction. By 08:12 UT, the disappeared IL showed up as a looplike dimming region, while another dimming region, "D," appeared around the eastern IL end. During the eruption, the leglike features near this end underwent clockwise rotations (*black arrows*), while those around the western IL end (*white arrows*) clearly

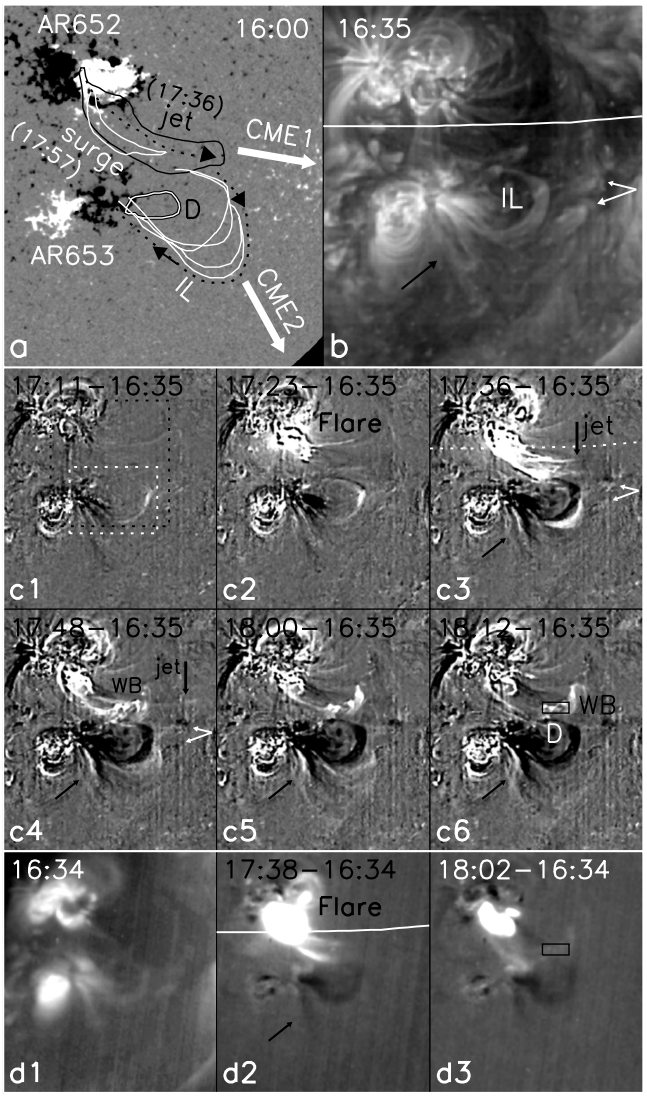

FIG. 1.—(*a*) MDI magnetogram. (*b*) EIT 195 Å and SXI SXR (panel *d*1) direct images before the flare, in which the loop-like structure, "IL." is clearly seen. Panels *c*1–*c*6 (*d*2 and *d*3) show EIT 195 Å (SXI SXR) fixed-base difference images. "D" and "WB" mark the dimming region near the eastern IL end and the weak brightenings around the western IL end, respectively. The black (white) thin arrows indicate the leglike features near the two IL ends. The white lines in panels *b*, *c*3, and *d*2 indicate the solar equator, and the black vertical arrows in panels *c*3 and *c*4 indicate the transequatorial jet that went beyond the western IL end. In (*a*), the outlines of the jet, the surge, D, and the outermost edge of the erupting IL are plotted: the dashed black curves with arrows indicate the field line directions in the jet and the erupting IL, and the thick white arrows indicate the eruptive directions of the two CMEs. The black (white) box in panel *c*1 indicates the FOV of Fig. 2 (Fig. 3). The FOV is 900″ × 1020″.

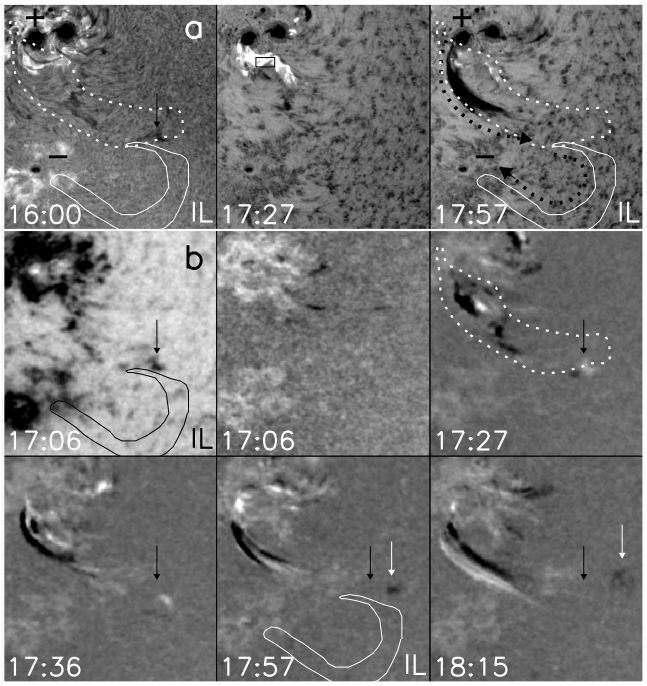

FIG. 2.—(*a*) BBSO Hα and (*b*) MLSO/CHIP He I 10830 Å images. The first frame in (*a*) ([*b*]) is the Hα center (He I 10830 Å intensity) image, while the others are Hα blue-wing (He I 10830 Å velocity) images. The black arrows indicate the initial position of the dark feature near the western IL end, while the white arrows indicate its current position. The outlines of the IL (the jet) determined from the 16:35 UT (17:36 UT) 195 Å image are plotted as solid (dashed) contours. The plus/minus sign marks the corresponding positive/negative magnetic polarity in the photosphere, and the field line directions of the surge and the IL as in Fig. 1 are also plotted. The FOV is $500'' \times 530''$.

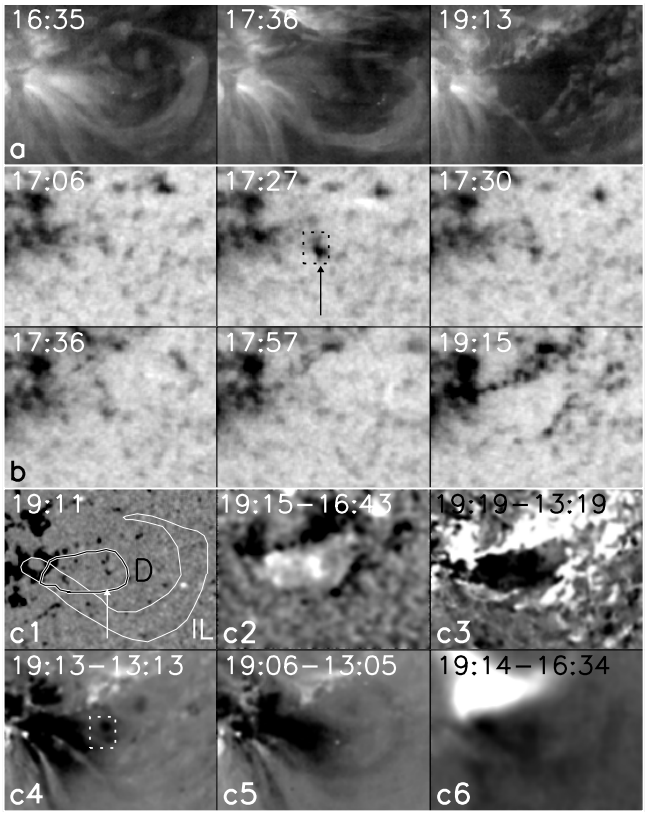

FIG. 3.—(*a*) EIT 195 Å and (*b*) He I 10830 Å intensity images. (*c*1) MDI magnetogram, (*c*2) He I 10830 Å, (*c*3) EIT 304, (*c*4) 195, (*c*5) 284 Å, and (*c*6) SXI SXR difference images. The arrows indicate the short-lived He I 10830 Å dark patch. The outlines of D and IL as in Fig. 2 are also plotted. The FOV is $370'' \times 280''$.

showed activations. This possibly indicates that the interconnecting loop system wholly erupted along with the IL. In SXI SXR observations, the jet and the IL eruption were also seen and showed consistent evolution.

Consistent with the previous result that a chromospheric surge and a coronal jet can be coexistent phenomena in the same plasma ejection (Shibata et al. 1992; Yoshimura et al. 2003), a surge, the chromospheric counterpart of the jet, was also observed in BBSO Hα (Fig. 2*a*) and MLSO He I 10830 Å (Fig. 2*b*) in this event. However, the surge showed different evolution from the jet in time and space (Schmieder et al. 1994; Chae et al. 1999; Jiang et al. 2007a). Its first appearance at about 17:27 UT was later than that of the jet at 17:23 UT. Despite ejecting from the same preceding part of AR 10652 with positive polarity, they did not share the same footpoint, and the surge was shorter and thinner than the jet and only traced its eastern edge. This can be seen from the outlines of the 17:36 UT 195 Å jet and the 17:57 UT Hα surge near its maximum phase plotted in Figures 1*a* and 2. However, a more interesting finding is that a dark feature, which was very close to the western IL end and can be clearly seen in the Hα center and He I 10830 Å intensity images in Figure 2, was disturbed by the surge. Its motion was obvious in the He I 10830 Å velocity images after the surge start, and the He I 10830 Å movie reveals that it eventually erupted. The jet outlines plotted in Figure 2 indicate that the southern edge of the longer and wider jet directly hit at the western IL end and this dark feature. Therefore, this disturbance gives further evidence for the occurrence of magnetic interaction around the western IL end. Figure 3 presents the close-up view of the dimmings. In direct EIT 195 Å images, the D formed during the IL eruption and was clearly discernible after the IL disappearance. In He I 10830 Å intensity images, as a common characteristic of dimming formation (Jiang et al. 2003, 2007c; de Toma et al. 2005), the D was formed over the region of chromospheric network. During the early formation phase, a small dark patch appeared on the region where the D would form, and persisted for only a few minutes. In Figure 3*c* we compare the fixed-base difference images at He I 10830 Å, EIT 304, 195, and 284 Å, and SXI SXR. The D, as dimming in EUV and X-ray and brightening in He I 10830 Å, was clearly visible and showed similar location and shape in these lines covering a wide temperature range, suggesting that it was due to a loss in density rather than a decrease in temperature in the coronal plasma (Thompson et al. 1998). However, the looplike dimming did not present in 304 Å and He I 10830 Å, clearly indicating that it was simply due to the IL disappearance. The outlines of the IL and the D determined from the 19:19 UT 304 Å image plotted in Figure 1*a* and panel *c*1 in Figure 3 show that the D was located in negative-polarity region near the eastern IL end.

Two successive CMEs, "CME1" and "CME2," were observed by LASCO within 2 hr of the time of the event. CME1 (CME2) first appeared in the C2 field of view (FOV) at 17:54 UT (19:31 UT), and later in the C3 FOV at 18:18 UT (19:42 UT) as a (another) ragged, arcade-like bright front. Figure 4 shows the structures and evolutions of the two CMEs. According to S. Yashiro's measurements, the CME1 (CME2) had a width of 142° (100°), and a central position angle (P.A.) of 260° (209°). Therefore, their eruption directions determined from the central P.A. (see Fig. 1*a*) were nearly along those of the flare-associated jet and the IL, respectively. The application of first-order (second-order) polynomial fitting to height-time (H-T) points of the CME1 front at P.A. 256°

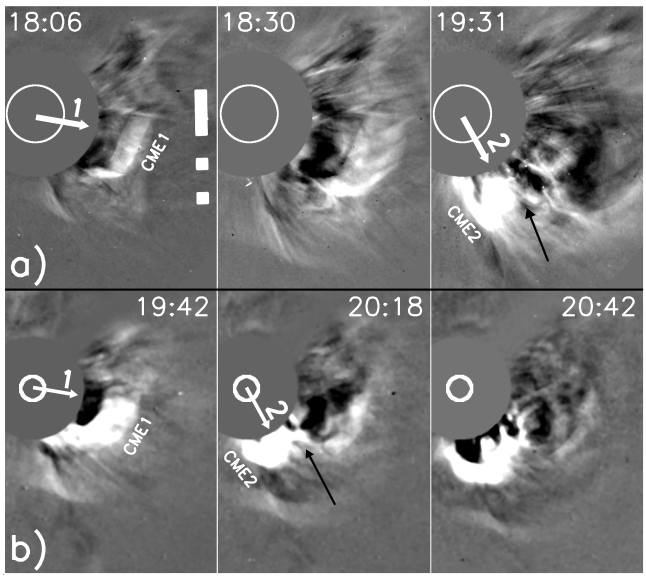

FIG. 4.—(*a*) LASCO C2 and (*b*) C3 difference images showing the evolution of the two CMEs. The white arrows indicate their eruptive directions, and the black arrows indicate the intersection of their bright fronts.

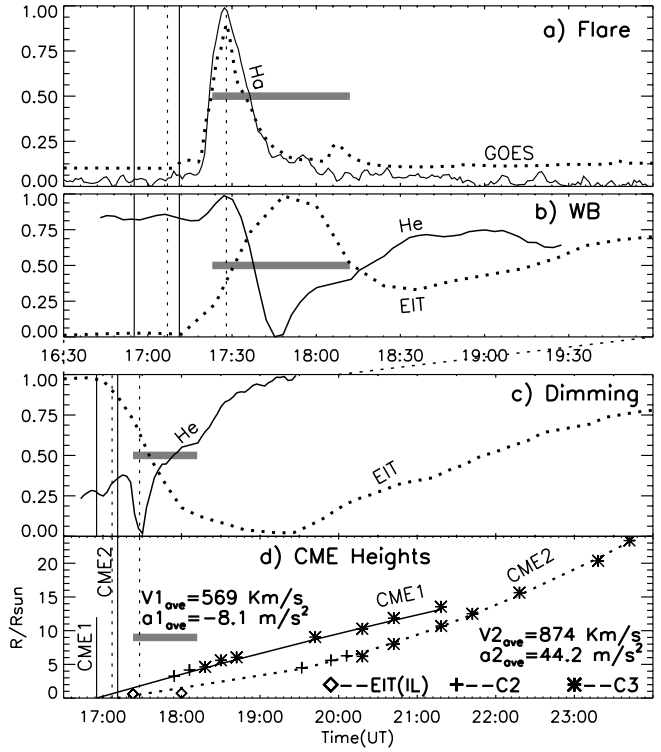

FIG. 5.—Time profiles of *GOES-10* 1-8Å SXRs (panel *a*, *dashed lines*), which are displayed in an arbitrary unit to fit in the panel. The light curves of Hα blue-wing intensities (panel *a*, *solid lines*) in an area centered on the flare (Fig. 2, *black boxes*), and EIT 195 Å (panels *b* and *c*, *dashed lines*) and He I 10830 Å (panels *b* and *c*, *solid lines*) intensities in areas centered on WB and D (boxes in panels *c6* and *d3* in Figs. 1 and 3, respectively), which are computed from the intensity integrated and normalized over these regions. (*d*) Heights of the fronts of the two CMEs as the function of time, and the back extrapolations by the use of second-order polynomial fitting. The vertical dashed bars indicate the start and peak times of the flare, the vertical solid bars indicate the extrapolated onset times of the two CMEs, and the horizontal bars indicate the duration of the IL eruption.

gives an average speed (acceleration) of 569 km s^{-1} (−8.1 m s^{-2}), while for CME2 front at P.A. 187°, 874 km s^{-1} (44.2 s^{-2}). Thus, the CME2 had larger speed and acceleration than that of the CME1. Since their angular difference was only 51° in central P.A. and they were so close in time, it is expected that the fast CME (CME2) can approach the slow one (CME1). In Figure 4 (*black arrows*) an intersection area appeared between them as the first appearance of the CME2 at 19:31 UT and can be seen in the C3 FOV until 20:18 UT. This intersection, which was very similar to an example shown by Moon et al. (2003), may be due to a mere overlap of the two CMEs along the line of sight or an interaction of the CME2 with one of legs of the CME1 (Gopalswamy et al. 2002b). This was clearly different from the "CME cannibalism" shown by Gopalswamy et al. (2001, 2002a), in which a following fast CME caught up and interacted with a preceding slow one so as to form a single CME since they roughly had the same central P.A. or the size of the fast CME was large enough. In this case, we see that the CME2 did not overtake or go beyond the whole CME1 inside the C3 FOV all along. By applying second-order polynomial fitting, back extrapolation of the CME1 (CME2) front from the H-T plots to the eruptive location yields an estimate of the CME1 (CME2) onset time near 16:55 (17:11) UT, which is very close to the start time of the flare (the IL eruption) at 17:07 (17:23) UT. The spatial and temporal consistencies strongly suggest that the CME1 initiation was closely related to the flare, while the CME2 was due to the IL eruption. In this sense, the two CMEs should be considered as a sympathetic pair since the flare and IL eruption occurred in different positions and were physically connected by the flare-associated jet.

In Figure 5 the *GOES* SXR flux, the light curves of EIT 195 Å (He I 10830 Å) intensities in the WB and the D and Hα blue-wing intensities in the flare core are plotted. The extrapolated CME onset times, and the average speeds (accelerations) of the CME fronts from the first (second) order polynomial fitting are also indicated. It is clear that the Hα flare light curves were similar to the *GOES* 1-8 Å SXR flux profiles. During the IL eruption, the He I 10830 Å intensities in the WB showed an obvious increase, while in the D, first a decrease, due to the dark patch appearing during the early D formation phase, and then an obvious increase was seen. Correspondingly, the 195 Å intensities showed an increase (decrease) in the WB (D), which occurred nearly simultaneously with the extrapolated CME2 onset time. The obvious changes of EUV intensities in both WB and D were slightly earlier than that of He I 10830 Å, which may be due to their different atmospheric respondence and image cadence. In Figure 5*d* two H-T points of the erupting IL at 17:23 and 18:00 UT are also plotted. They are very close to the extrapolated curves of the CME2, also implying the close relationship between the IL eruption and the CME2.

4. CONCLUSIONS AND DISCUSSION

We present the first evidence for occurrence of magnetic interaction between a jet and the IL that acted as driving agent of the sympathetic CMEs. The interaction was manifested as the direct impact of the jet edge with one IL end, as well as the weak brightenings and the disturbance of the dark feature adjacent to this end. Different from the event studied by Khan & Hudson (2000), the IL eruption was directly observed and clearly due to such interaction. Therefore, both the eruptions in the opposite hemisphere, the flare (the IL eruption) in the northern (southern) hemisphere, were linked together by the transequatorial jet originating from the flare, and it is evidence that they were closely associated with the two interdependent CMEs that sequentially occurred within 2 hr. We believe that this is the most obvious and certain example of sympathetic CME pair ever observed. It is

not uncommon that plasma ejections in X-ray (Nitta & Akiyama 1999; Kim et al. 2005) and in Hα (Liu et al. 2005) can be tightly associated with CMEs. In this case, only the jet edge impacted on the IL, while its major portion appeared to eject to space. Therefore, it is not surprising that the flare and associated jet could be related to the CME1. Consistent with the observations of Khan & Hudson (2000), however, our observations reveal that IL can also erupt to form a CME. The CME2 was most likely due to the IL eruption, i.e., the CME2 was nothing other than the erupting IL. If so, as suggested by Khan & Hudson (2000), the material of the CME2 was seen in the EUV and SXR images prior to its ejection. Since ILs are more common coronal structures than the TILs on the Sun (Chase et al. 1976), it is expected that IL eruptions should be more often observed than TIL eruptions.

Similar to the event of Khan & Hudson (2000), the looplike dimming in this case was also simply resulted from the IL disappearance after its eruption. However, the formation of the D provided some important implications for the IL eruption and the CME2, which have not been reported previously. Since the D formed in the course of the IL eruption and located on unipolar magnetic-field region nearby one IL end, it probably represented the evacuated feet of the IL that were caused by the expansion, or even the opening, of the IL's magnetic field lines, just like the case of bipolar double dimmings in some eruptive events (Jiang et al. 2003, 2007b, 2007c; de Toma et al. 2005). The short-lived He I 10830 Å darkenings implied that the plasma heating may occur during the early phase of the D formation. Therefore, in addition to the erupting IL itself, the lost mass originating from its footpoints could also provide mass to the CME2.

Wang et al. (2001) showed that an IL can be activated by a surge. The surge quickly turned into a set of disturbances, and they suggested that such disturbances may represent mass transfer and cause the transport of field lines. In our case, no similar disturbance coming from the surge was observed, and the detailed mechanism of the jet/IL interaction is still open. For example, does such interaction change the linkage of the IL field lines to the photosphere? Does the jet mass pile up and the magnetic reconnection really occur at the impacting site? Further observations and theoretical work will be essential to answer these questions.

We thank an anonymous referee for many constructive suggestions and thoughtful comments, which improved the quality of this paper. We are grateful to the observing staff at BBSO for making good observations. He I 10830 Å data were provided by the High Altitude Observatory of the National Center for Atmospheric Research, which is sponsored by the National Science Foundation. We thank the *GOES* SXI team, the *SOHO* MDI, EIT and LASCO teams for data support. This work is supported by the Natural Science Foundation of China under grants 10573033 and 40636031 and by the 973 program (2006CB806303).

REFERENCES

Aschwanden, M. J. 2004, Physics of the Solar Corona: An Introduction (New York: Springer)
Balasubramaniam, K. S., Pevtsov, A. A., Neidig, D. F., Cliver, E. W., Thompson, B. J., Young, C. A., Martin, S. F., & Kiplinger, A. 2005, ApJ, 630, 1160
Brueckner, G. E., et al. 1995, Sol. Phys., 162, 357
Chase, R. C., Krieger, A. S., Svestka, Z., & Vaiana, G. S. 1976, in Space Research XVI, ed. M. J. Rycroft (Berlin: Akademie), 917
Chae, J., Qiu, J., Wang, H., & Goode, P. R. 1999, ApJ, 513, L75
Cheng, J., Fang, C., Chen, P., & Ding, M. 2005, Chinese J. Astron. Astophys., 5, 265
Chertok, I. M., Grechnev, V. V., Hudson, H. S., & Nitta, N. V. 2004, J. Geophys. Res., 109, A02112
Cliver, E. W., & Hudson, H. S. 2002, J. Atmos. Terr. Phys., 64, 231
Delaboudinière, J.-P., et al. 1995, Sol. Phys., 162, 291
Delannée, C., & Aulanier, G. 1999, Sol. Phys., 190, 107
de Toma, G., Holzer, T. E., Burkepile, J. T., & Gilbert, H. R. 2005, ApJ, 621, 1109
Glover, A., Harra, L. K., Matthews, S. A., & Foly, C. A. 2003, A&A, 400, 759
Gopalswamy, N., Yashiro, S., Kaiser, M. L., Howard, R. A., & Bouegret, J.-L. 2001, ApJ, 548, L91
———. 2002a, Geophys. Res. Lett, 29, 106
Gopalswamy, N., Yashiro, S., Michalek, G., Kaiser, M. L., Howard, R. A., Reames, D. V., Leske, R., & Von Rosenvinge, T. 2002b, ApJ, 572, L103
Harra, L. K., Matthews, S. A., & van, Driel-Gesztelyi, L. 2003, ApJ, 598, L59
Hill, S. M., et al. 2005, Sol. Phys., 226, 255
Hudson, H. S., & Cliver, E. W. 2001, J. Geophys. Res., 106, 25199
Jiang, Y., Chen, H., Li, K., Shen, Y., & Yang, L. 2007a, A&A, 469, 331
Jiang, Y., Chen, H., Shen, Y., Yang, L, & Li, K. 2007b, Sol. Phys., 240, 77
Jiang, Y., Ji, H., Wang, H., & Chen, H. 2003, ApJ, 597, L161
Jiang, Y., Yang, L., Li. K., & Ren, D. 2007c, ApJ, 662, L131
Jiang, Y., Yang, L., Li. K., & Shen, Y. 2007d, ApJ, 667, L105
Kahler, S. W. 1991, ApJ, 378, 398
Khan, J. I., & Hudson, H. S. 2000, Geophys. Res. Lett, 27, 1083
Kim, Y.-H., Moon, Y.-J., Cho, K.-S., Kim, K.-S., & Park, Y. D. 2005, ApJ, 622, 1240
Liu, Y., Su, J., Morimoto, T., Kurokawa, H., & Shibata, K. 2005, ApJ, 628, 1056
Lyons, M. A., & Simnett, G. M. 1999, Sol. Phys., 186, 363
MacQueen, R. M., Blankner, J. G., Elmore, D. F., Elmore, D. E., Lecinski, A. R., & White, O. R. 1998, Sol. Phys., 182, 97
Moon, Y.-J., Choe, G. S., Park, Y. D., Wang, H., Gallagher, P. T., Chae, J., Yun, H. S., & Goode, P. 2002, ApJ, 574, 434
Moon, Y.-J., Choe, G. S., Wang, H., & Park, Y. D. 2003, ApJ, 588, 1176
Nitta, N., & Akiyama, S. 1999, ApJ, 525, L57
Nitta, N., & Hudson, H. S. 2001, Geophys. Res. Lett, 28, 3801
Pevtsov, A. A. 2000, ApJ, 531, 553
Pohjolainen, S., et al. 2001, ApJ, 556, 421
Reale, F. 1999, Sol. Phys., 190, 139
Saito, T., Sun, W., Deehr, C. S., & Akasofu, S.-I. 2007, J. Geophys. Res., 112, 5102
Schmieder, B., Golub, L., & Antiochos, S. K. 1994, ApJ, 425, 326
Scherrer, P. H., et al. 1995, Sol. Phys., 162, 129
Shibata, K., et al. 1992, PASJ, 44, L173
Simnett, G. M., & Hudson, H. 1997, in Proc. 31st ESLAB Symp., Correlated Phenomena at the Sun, in the Heliosphere and in Geospace, ed. A. Wilson (ESA-SP-415; Noordwijk: ESA), 437
Steinegger, M., et al. 2000, in The Solar Cycle and Terrestrial Climate, ed. A. Wilson (ESA SP-463; Noordwijk: ESA), 617
Svestka, Z. 2001, Space Sci. Rev., 95, 135
Thompson, B. J., Plunkett, S. P., Gurman, J. B., Newmark, J. S., St. Cyr, O. C., & Michels, D. J. 1998, Geophys. Res. Lett, 25, 2465
Wang, H., Chae, J., Yurchyshyn, V., Yang, G., Steinegger, M., & Goode, P. R. 2001, ApJ, 559, 1171
Wang, J., Zhang, Y., Zhou, G., Harra, L. K., Williams, D. R., & Jiang, Y. 2007, Sol. Phys., 244, 75
Yoshimura, K., Kurokawa, H., & Shine, R. 2003, PASJ, 55, 313
Zhang, J., & Wang, J. 2002, ApJ, 566, L117
Zhou, G., Wang, J., & Zhang, J. 2006, A&A, 445, 1133